Thermal Properties and Ionic Conductivity in Salt-Containing POEM/PEO Polymer Blend Electrolytes

Marissa Gallmeyer[a], Hsin-Ju Wu[a], William Breining[b], David M. Lynn[a,b], Whitney S. Loo[a]*

[a] University of Wisconsin-Madison Department of Chemical and Biological Engineering, Madison WI, 53706

[b] University of Wisconsin-Madison Department of Chemistry, Madison WI, 53706

*Corresponding author email: wloo@wisc.edu

Abstract

Polymer blend electrolytes are one possible pathway to developing solid electrolytes with improved properties when compared to the widely studied poly(ethylene oxide) (PEO) and lithium bis(trifluoromethanesulfonyl)imide (LiTFSI) system. However, many previously studied polymer blend electrolytes are not fully miscible at varying salt concentrations across the full blend composition window. In this study, we design a polymer blend electrolyte system that is fully miscible and characterize its thermal and ion transport properties. Poly (oligo ethylene oxide methacrylate) (POEM) is an ion conducting polymer with ethylene oxide side chains that can be varied in length. Our polymer blend electrolyte system contains PEO, POEM, and LiTFSI where we vary POEM monomer chemistry to determine the effect of side chain length and molecular weight on blend properties. All PEO/POEM/LiTFSI blends were miscible, regardless of POEM monomer structure, blend composition, or salt concentration. We characterize the blend properties using differential scanning calorimetry (DSC) and variable-temperature electrochemical impedance spectroscopy (EIS). Using the blend glass transition temperature and a modified Fox Equation, we are able to determine the salt partitioning within the system and quantify changes in the segmental dynamics of the polymer blend. We find that while Li ions are primarily solvated by PEO, the POEM

monomer structure determines the extent. Through EIS, we find that longer side chains more easily solvate the Li ions and have higher ionic conductivities. This study shows that engineering the solvation structure and segmental dynamics of salt-doped polymer blend can lead to developing electrolytes with improved ion transport properties for battery applications.

Keywords: polymer electrolytes, polymer blends, segmental dynamics, ion transport, glass transition

Introduction

The replacement of liquid electrolytes, commonly used in current lithium-ion batteries (LIBs), with solid electrolytes would provide a pathway for the development of more chemically and thermally stable, energy dense batteries that would meet the growing demands for safe and efficient energy storage. [1–4] In addition, solid electrolytes would allow for the use of lithium metal batteries, which are more energy dense than LIBs, due to their ability to suppress Li dendrite growth and form more stable interfaces with Li metal as compared to liquid electrolytes.[5–7] Solid polymer electrolytes (SPEs) are being currently explored for these applications where poly(ethylene oxide) (PEO) doped with lithium bis(trifluorosulfonylimide) (LiTFSI), PEO/LiTFSI, is the most well studied and understood SPE.[2,8–13]

It is generally understood that the motion of lithium ions in SPEs is reliant on the segmental dynamics of the polymer, which acts as the solvent.[2,7,14–17] Therefore, increasing the segmental dynamics of salt-containing polymers is one engineering strategy to increase their ion transport properties. One approach to accomplish this is to add small molecule plasticizers to the electrolytes. The addition of poly(ethylene glycol) (PEG), which refers to low molecular weight PEO, to

high molecular weight PEO has been shown to increase its ionic conductivity.[18] However, the hydroxyl end groups of PEG react with lithium metal, making them unfit for use in lithium metal batteries.[2] Other studies have considered the use of ethylene carbonate and propylene carbonate as plasticizers, which are commonly used as liquid electrolytes for LIBs.[2,19,20] While these liquid plasticizers are able to increase the ionic conductivity by several orders of magnitude, the chemical stability required for safety and fast battery recharging as well as the mechanical properties needed to suppress dendrites are both reduced.[2]

Polymer blend electrolytes have emerged as promising candidate materials given that their composite nature allows for optimization of electrolyte properties including chemical stability and mechanical properties. Previous work by Zhu et al. studied blends of poly(cyanoethyl glycidyl ether) and poly(allyl glycidyl ether) blended with Li salts. They found that the phase behavior of the blends was dependent on salt concentration and that immiscible blends had significantly lower ionic conductivity than miscible blends.[21] It is well established that most electrolytes will form salt concentration gradients under battery operation.[22] Therefore, in order to maximize ion transport properties, the electrolytes must be miscible at a wide range of salt concentrations in order to remain homogenous. Gao et al. considered a blend of PEO and poly(1,3,6-trioxocane) (P(2EO-MO)).[23] While blends of PEO/P(2EO-MO)/LiTFSI were found to be miscible at high salt concentrations, regions of the phase diagram are immiscible at low salt concentrations making these blends non-ideal electrolyte systems. Other systems explore PEO and poly(methyl methacrylate) (PMMA) blend electrolytes as PEO and PMMA are miscible in the absence of salt.[8,14,23–25] Similar to previous studies of polymer blend electrolytes, PEO/PMMA/LiTFSI blends are not fully miscible, with large regions of the phase diagram indicating immiscibility. [24,25]

In this work, we propose to blend PEO with poly(oligo ethylene oxide methacrylate) (POEM), a polymer that contains a methacrylate backbone with variable-length ethylene oxide (EO) side chains and is characterized by one T_g value that represents the segmental dynamics of the full repeat unit.[26] Previous work has demonstrated that while there is a difference in the segmental dynamics between the rigid backbone and flexible side chain of POEM, it manifests as a gradient as opposed to two distinct regimes. Through atomistic simulations, Deng and coworkers showed that the EO units closest to the backbone have the slowest degree of segmental motion and each subsequent EO unit has increasing degrees of segmental mobility.[27] In fact, for a POEM polymer with nine EO units on its side chain, the EO units furthest away from the backbone have faster segmental dynamics than compared to linear PEO repeat units.[26] In addition, the EO side chains should improve the miscibility with PEO and provide faster segmental dynamics, regardless of blend composition or salt concentration.[26] Given the requirement of five to six EOs to solvate one Li ion, by varying the side chain length, we can explore how the solvation environment impacts the blend segmental dynamics and the resulting ionic conductivity. In this study, we investigate how POEM side chain length and molecular weight impact the glass transition temperature (T_g) with differential scanning calorimetry (DSC). All blends studied show only one T_g value indicating miscibility across the phase diagram. Based on the measured T_g values, we quantify the salt partitioning in the system, i.e., the fraction of salt that is solvated by each polymer component, and find that the LiTFSI favors solvation by the PEO rather than the POEM. In addition, we show that ion solvation by POEM is highly dependent on monomer structure. Variable-temperature electrochemical impedance spectroscopy (EIS) is then used to measure the ionic conductivity of each electrolyte. We find that the blends with longer POEM side chains perform better than those with shorter side chains, with some blend electrolytes even displaying the same ionic conductivity as

PEO/LiTFSI. We further investigate how blend properties, such as segmental dynamics and ion solvation structure, affect ionic conductivity by calculating the reduced conductivity. Based on our findings, we believe that polymer blend electrolytes provide a unique materials engineering strategy to optimize electrolyte properties.

Methods and Materials

Materials

PEO with a molecular weight of 30 kg/mol and polydispersity index (PDI) of 1.01 was purchased from Polymer Source. Oligo ethylene oxide methyl ether methacrylate (OEM) monomers with side chain lengths of 2, 5, and 9 ethylene oxide units (Mn = 188, 300, and 500 g/mol, respectively), 99.9% anhydrous toluene, 99.9% anhydrous acetonitrile, HPLC grade tetrahydrofuran (THF), >97% (HPLC) 2-cyano-2-propyl benzodithioate (CPBD) reversible addition-fragmentation chain-transfer (RAFT) agent, 2,2'-azobisisobutyronitrile (AIBN), basic alumina, dimethyl sulfoxide-d_6 (99.9 atom % D, contains 0.03% (v/v) tetramethylsilane (TMS)), and 99.95% trace metal basis lithium bis(trifluorosulfonylimide) (LiTFSI) were purchased from Sigma-Alderich. PEO and LiTFSI were dried in the antechamber of an argon glovebox under active vacuum at room temperature for over 48 hours prior to use. All reagents were used as received without further purification unless specified otherwise.

POEM Polymer Synthesis

POEM variants were synthesized via RAFT polymerization of the OEM monomers through the following general method. An appropriately sized Schlenk flask equipped with a Teflon-coated stir bar was cleaned in a base bath, washed with deionized water and acetone, and then dried in a 160 °C glassware oven. The inhibitor was removed from the OEM monomer by passing the monomer

through a basic alumina pipette column one time. All reagents and solvent were then added to the Schlenk flask. CPBD was used as the RAFT agent. Solvent was added at approximately 1 molal with respect to the monomer. The exact proportions of OEM monomer, CPBD, AIBN, and toluene for each polymer can be found in Table S1. The Schlenk flask was then degassed using three rounds of the freeze-pump-thaw method. Liquid nitrogen was used to freeze the polymerization solution, at which point the Schlenk flask was opened to vacuum. After pulling a vacuum on the Schlenk flask, the flask was closed to vacuum and the solution was allowed to thaw. After the third freeze-pump-thaw cycle, no bubbles were observed in solution during the thaw step. The Schlenk flask was then backfilled with dry nitrogen to give the polymerization an inert atmosphere. The tube was then lowered into a 70 ºC oil bath for 24 hours after which the polymerization was quenched by placing in an ice bath and exposing to air. Polymer was purified by dissolution in THF and precipitations into approximately 90 mL of cold hexanes. Three rounds of purification were performed. Polymers were dried at 50 ºC under vacuum for at least 24hrs. Samples were then analyzed via ^{1}H nuclear magnetic resonance spectroscopy (NMR) and gel permeation chromatography (GPC) to verify purity. If found to be impure, additional purification rounds and drying were completed.

Electrolyte Preparation

Polymers were dried in the glovebox antechamber under active vacuum at room temperature in the glovebox antechamber for 24hrs before being transferred to an argon glovebox. They were stored in the glovebox freezer. Polymer blends were created by making stock solutions of PEO, POEM, and LiTFSI in acetonitrile at 25 mg/mL concentration. Covered solutions were allowed to stir over night to ensure full dissolution. Stock solutions were pipetted into jars in the appropriate amounts for each blend or electrolyte. All blending ratios unless otherwise denoted, are a ratio of

[EO_{PEO}]/[EO_{POEM}] and r = [LiTFSI]/[EO]. End groups were neglected in all calculations. The solutions were allowed to stir uncovered until all solvent had evaporated and then further dried in the vacuum oven under ~60 ºC for at least 24hrs.

Polymer Characterization

Purity was confirmed with further characterization by ^{1}H NMR using a Bruker 500 MHz Avance III spectrometer equipped with a DCH cryoprobe. NMR spectra were recorded with Bruker TopSpin 3.5.6 and analyzed using MestReNova. ^{1}H NMR spectroscopy was performed using a relaxation delay (d1) of 1s. NMR chemical shifts are shown in ppm and are referenced to TMS at δ = 0.00 ppm. Glass transition temperatures (T_g) were found via Differential Scanning Calorimetry (DSC). The heating cycle consisted of equilibration at 120 ºC followed by a cooling ramp of 5°/min to -80 °C and a heating ramp of 10 º/min to 120 ºC. This cycle was completed for a total of three repetitions. The T_g values used were from the third heating cycle. All samples have had only one T_g value, indicating full miscibility. GPC was used to determine the molecular weight of polymers on a Viscotek GPCmax-VE2001 (Viscotek Corp., Houston, TX) with THF as the mobile phase with a flow rate of 1.0 mL/min. An injection volume of 100µL was used and the run time was 45 minutes. The OmniSEC 4.5 software was used to process data taken by the refractive index detector. The molecular weights were determined using a calibration curve with known polystyrene (PS) standards.

Electrochemical Impedance Spectroscopy (EIS)

Electrical Impedance Spectroscopy (EIS) on pouch cells was used to measure ionic conductivity. Pouch cells were fabricated with two stainless steel shims as the electrodes with a silicon spacer with thickness of 0.020 inches to hold the electrolyte. Electrolyte was placed in the center of the

spacer such that it had good contact with both stainless-steel electrodes. The area of the polymer was 0.079173 cm^2. The electrode/electrolyte/electrode stack was sealed in aluminum pouch with nickel tabs on either side of the cell. The cell was annealed at 90 °C for 4 hours on a custom heating stage outside of the glovebox. It was then allowed to equilibrate at 30 °C prior to the first measurement. Measurements were taken upon heating in 10-degree increments after 20-minute equilibration periods. EIS was conducted on a BioLogic VSP-3e Potentiostat with a frequency range of 1 MHz to 100 mHz. An applied amplitude of 80 mV was used. Bulk resistance was found using an through the analysis tool in EC-Lab software. This value in conjunction with the thickness measured after EIS measurement was used to calculate the conductivity according to

$$\sigma = \frac{l}{AR_B} \tag{1}$$

Where σ is the ionic conductivity, l is the electrolyte thickness, A is the area of the electrolyte, and R_B is the bulk resistance obtained from the Nyquist plot. All reported conductivity values are the average of triplicate data. Error bars represent the standard deviations from the triplicate data.

Results and Discussion

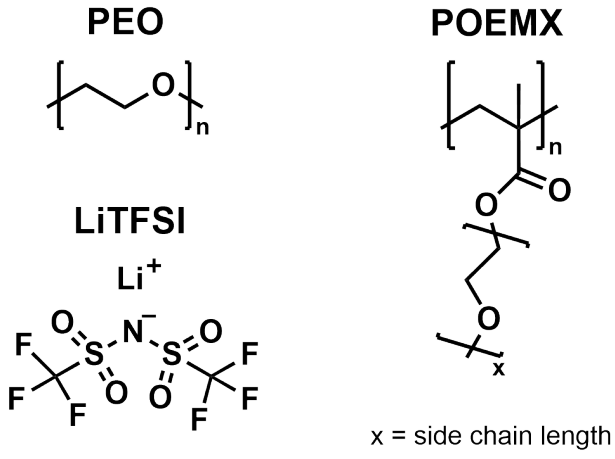

Figure 1. Chemical structures of poly(ethylene oxide) (PEO), poly(oligo ethylene oxide methacrylate) (POEM), and lithium bis(trifluoromethanesulfonyl)imide (LiTFSI).

Figure 1 shows the molecular structure of components of the polymer blend system: PEO, POEM, and LiTFSI. Specific variations of POEM will be denoted as POEMX-Y where X denotes the number of EOs in the side chain on each monomer and Y denotes the approximate molecular weight. The POEM was synthesized via RAFT polymerization (see the Methods and Materials for the general polymerization procedure used) and the PEO was purchased from Polymer Source. **Table 1** shows the full library of polymers included in this study and their relevant properties. The molecular weights of the POEM samples were chosen such that there were a consistent number of EO moieties per chain as well as a consistent number of POEMX repeat units, *n.* Blends are prepared by varying the composition of PEO and POEM based on the molar fractions of EOs in each polymer, $[EO_{PEO}]/[EO_{POEM}]$. For example, a 75/25 blend has 75 mol% of the EOs from PEO chains and 25 mol% of the EOs from POEMX-Y chains, which corresponds to a weight fraction of PEO, w_{PEO}, of 0.57 for blends prepared with POEM2-8 and 0.70 for blends prepared with POEM9-5. We refer to the blends by their blending ratio as w_{PEO} differs between blends prepared with different POEM polymers due to differences in the POEMX monomer molecular weights. Blend compositions range from 0/100 to 100/0. Salt concentration is quantified by *r,* which is the molar ratio of Li to EOs, r = [Li]/[EO], where the EOs from both PEO and POEM are taken into account ($[EO]=[EO_{PEO}]+[EO_{POEM}]$). The oxygens in the methacrylate backbone are known to not participate in ion solvation and are therefore not accounted for when calculating the value of r.[26,28] In this study, we limit our discussion to blends with r = 0 and 0.10 as all blends are amorphous at upon the addition of the appropriate amount of LiTFSI.

Table 1. Molar mass, size, dispersity, and monomer size of each polymer studied.

Polymer	x[a]	Mn (kg/mol)	n[b]	PDI
POEM9-5	9	5.8	12	1.17
POEM5-4	5	4.7	16	1.18
POEM5-7	5	7.3	20	1.29
POEM2-3	2	3.2	17	1.17
POEM2-8	2	8.2	44	1.20
PEO[*]	-	30	-	1.01

[a] Approximate number of ethylene oxide side chains on each monomer. [b] Average number of repeat units per polymer M_o/Mn. [*]Characterization provided by Polymer Source

Differential scanning calorimetry (DSC) was used to understand the effect of blend composition and salt concentration on the blend segmental dynamics. All blends contained only one identifiable T_g, indicating miscibility at all blend compositions and salt concentrations (full DSC profiles for all blends are included in the SI).[29] **Figure 2a** shows the T_g values for blends containing POEM9-5, PEOM5-7, and POEM2-8 at $r = 0$ as a function of w_{PEO}. The solid markers depict the T_g data while the lines are fits to the Fox equation given by[30]:

$$\frac{1}{T_g} = \frac{w_{PEO}}{T_{g,PEO}} + \frac{w_{POEM}}{T_{g,POEM}} \quad (2)$$

The T_g of the pure POEM, $T_{g,POEM}$ ($w_{PEO} = 0$), is highly dependent on monomer structure, where the T_g decreases as EO side chain length, X, increases. For example, the T_g of POEM9-5 and POEM5-7 is lower than that of pure PEO ($w_{PEO} = 1$ for all blends). Conversely, the T_g of POEM2-8 is higher than that of pure PEO despite having a significantly lower molecular weight. The high T_g value of POEM2-8 is due to the shorter EO side chains per monomer, and therefore, the rigid

methyl methacrylate backbone plays a larger role on its segmental dynamics as compared to the POEM9-5 and POEM5-7 polymers. Our results agree with previous studies on POEM polymers.[26] Additionally, the DSC traces for the POEM homopolymers exhibit very broad glass transitions due to the gradient of dynamics of the POEM repeat units (see Supporting Information). It is evident that the T_g's for blends prepared with POEM9-5 and POEM5-7 at $r = 0$ follow linear trends, which agrees with Fox Equation predictions.[30,31] Blends prepared with POEM2-8 displays slight positive deviations, indicating strong interactions between the POEM2 and PEO repeat units.[32]

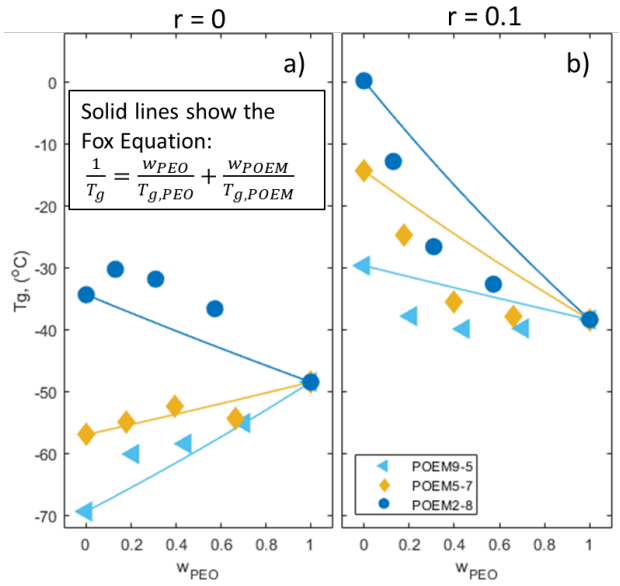

Figure 2. T_g of PEO/POEM blends containing POEM9-5, POEM5-7 and POEM2-8 (markers) with Fox Equation predictions (solid lines) for *a)* r = 0 and *b)* r = 0.1.

Figure 2b shows the T_g values for blends containing POEM9-5, PEOM5-7, and POEM2-8 at r = 0.1 as a function of w_{PEO}. The solid markers depict the T_g data while the lines are fits to the Fox equation (Eq 2). The addition of salt decreases the segmental dynamics, as indicated by an increase

in T_g for all blends and the presence of salt has a larger effect on the segmental dynamics of POEM than compared to that of PEO. At r = 0.1, all pure POEM electrolytes ($w_{PEO} = 0$) have a higher T_g than that of the pure PEO electrolytes. The relationship between POEM side chain length, X, and T_g is consistent for both the r = 0 and r = 0.10 samples. It's important to note that we have chosen to assume that the salt is evenly distributed between the PEO and POEM segments and therefore have not accounted for the presence of salt in our predictions using the Fox equation (i.e., the weight fractions employed in Figures 2a and 2b are equivalent). The salt-containing blends all display noticeable negative deviations from the Fox Equation predictions, *i.e.,* the measured T_g values are consistently below the model predictions. Data for blends prepared with POEM5-4 and POEM2-3 are included in the SI (Figure S27) and exhibit similar trends to the blends prepared with the other POEM polymers shown in **Figure 2**. Similar deviations from the Fox Equation have been observed in polymers containing certain plasticizers as well as in multiple polymer blends and has been attributed to attractive interactions introduced by non-ideal mixing.[33–35] In our system, we do not believe that the deviations from the Fox equation are due to non-ideal mixing between our polymer components as the solvation sites for the salt molecules are chemically identical between the PEO and POEM chains. Therefore, we hypothesize that the deviations from the Fox Equation indicate that the salt is not partitioning evenly between the PEO and POEM chains and that there is a larger amount of salt being solvated by PEO versus POEM. Therefore, we aim to modify the Fox Equation in order to quantify the partitioning of the salt. We do this by re-casting all parameters to include a dependence on r according to:

$$\frac{1}{T_g} = \frac{w_{PEO}(r_{PEO})}{T_{g,PEO}(r_{PEO})} + \frac{w_{POEM}(r_{POEM})}{T_{g,POEM}(r_{POEM})} \quad (3)$$

We can then use Eq 3 to solve for the salt concentration solvated by each polymer component, r_i. To obtain the expressions for both $T_{g,PEO}$ and $T_{g,POEM}$ as a function of r in Eq 3, we conducted DSC experiments to measure the T_g for homopolymer electrolytes of PEO and all POEM variants with r = 0.025 – 0.15. This data was fit to linear equations according to

$$T_{g,i} = mr_i + b \tag{3}$$

where $T_{g,i}$ is the T_g value for the homopolymer i, m and b are fitted constants and r_i quantifies the salt concentration for component i for i = PEO or POEM. At $r = 0.1$, PEO/LiTFSI is known to be fully amorphous.[9] Therefore, the fit for PEO is only based on data from r = 0.075 – 0.15 as below this salt concentration some crystalline features are found.[4] All fits and T_g data can be found in the Supporting Information. The weight fractions in Eq 3 were calculated according to

$$w_i(r_i) = w_i + xr_i \tag{4}$$

where w_i is the weight fraction of component i in the absence of salt, x is a side chain length dependent constant, and r_i is the r-value for component i. Then, using the known blend T_g values from **Figure 2b** and constraining the mass balance of polymer and salt to ensure consistency, it is possible to solve the system of equations for each of the blend electrolytes and determine the salt concentration solvated by each polymer component, r_{PEO} and r_{POEM}.

Figure 3a shows r_{PEO} for the POEM9-5, POEM5-7 and POEM2-8 as a function of w_{PEO}, where the dashed line at r = 0.1 represents the assumption of even salt partitioning between the PEO and POEM chains. As expected, r_{PEO} values are all above r = 0.1, indicating that the salt is preferentially solvated by the PEO chains. It is instructive to examine how blend composition affects r_{PEO} for each POEM variant individually. For POEM9-5 (triangles), r_{PEO} decreases with increasing w_{PEO}. For blends with low compositions of PEO, 25/75, the salt prefers the minority component

(PEO), which significantly increases r_{PEO} compared to the expected value as the PEO chains become enriched in salt compared to the POEM chains. Conversely, for blends with high compositions of PEO, 75/25, the salt prefers the majority component and therefore, the r_{PEO} is closer to that of the expected $r = 0.1$ value. A similar trend is observed in the POEM5-4 blends (Figure S34). We see different trends in r_{PEO} as a function of blend composition for PEOM5-7 (diamonds), where r_{PEO} follows the expected trend for 50/50 and 75/25 blends. However, at low compositions of PEO, 25/75, r_{PEO} is significantly lower than what was observed for POEM9-5. These deviations indicate that the Li solvation for these majority POEM blends is distinct from that of the other samples. Unique behavior was observed for the blends prepared with POEM2-8 and will be discussed later.

Figure 3b shows the calculated r_{POEM} as a function of w_{PEO}. The values of r_{POEM} fall below $r = 0.10$ for all blends studied. For blends prepared with POEM9-5 and POEM5-7, r_{POEM} decreases as the blend composition is changed from 25/75 to 50/50 and r_{POEM} remains fairly constant between blend compositions 50/50 and 75/25. The dependence on blend composition is weakest for POEM9-5 (triangles), which agrees with previous results that show that POEM polymers with longer EO side chains are better at solvating Li ions[26,27]. For blends prepared with POEM5-7 (diamonds), at compositions 50/50 and 75/25, r_{POEM} is significantly lower than that of POEM9-5 ($r_{POEM} < .025$), indicating that almost all of the salt is solvated by PEO chains. Previous work has used simulations to demonstrate that the side chain length of POEM affects the Li ion solvation environment.[27] Each Li ion requires six EOs to form a solvation shell.[17,26,36] Therefore, simulations have shown that while one monomer of POEM9 can solvate a Li ion in similar ways as a PEO chain, POEM5 requires at least two monomers, the use of two independent POEM5 chains, or a POEM5 monomer and PEO molecule to solvate a Li ion.[26] POEM2 requires an even more complex solvation structure that requires multiple distinct polymers and monomers. Therefore, we

hypothesize that when r_{PEO} approaches the value of r_{POEM} such as with the 25/75 blends for POEM5-7, some portion of the Li ions are being co-solvated by PEO and POEM. As w_{PEO} increases, r_{POEM} decreases, indicating that there is less co-solvation occurring and that PEO is solvating a majority of the LiTFSI molecules independently as PEO becomes the majority component. Our results also indicate that the molecular weight of POEM plays an important role in salt partitioning. The POEM5-4 blends behaved similarly to PEOM9-5 where the r_{PEO} value decreased with increasing w_{PEO} indicating that the PEO chains were solvating the majority of the Li ions, see Figure S34 in the Supporting Information. Conversely, POEM5-7 exhibited a high degree of co-solvation. It is interesting that we observe this difference in blend behavior at such small differences in molecular weight of POEM5-4 and POEM5-7. Therefore, POEM with higher molecular weights are able to form more homogeneous blends with PEO and can more actively participate in Li ion co-solvation.

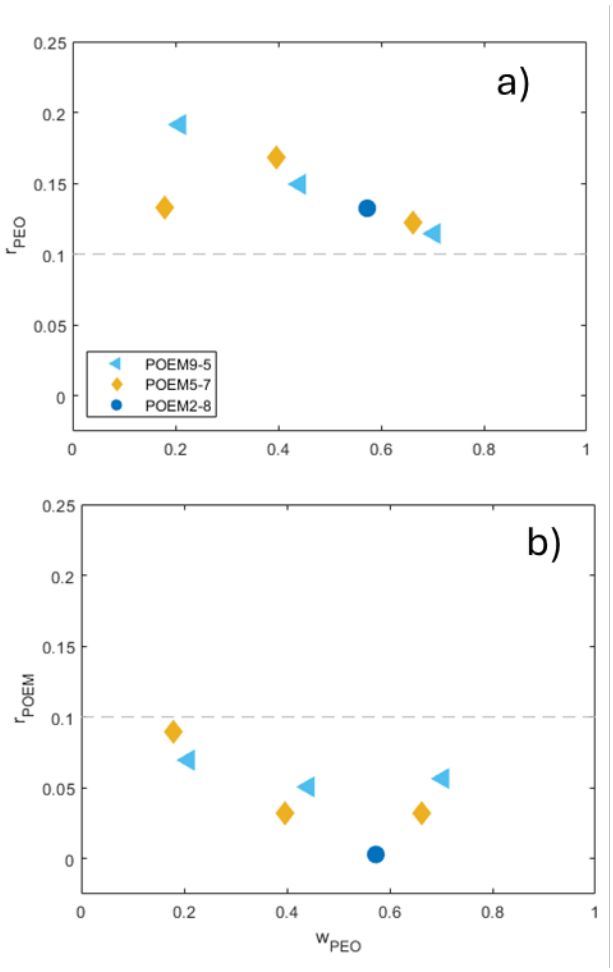

Figure 3. Calculated r_i for the a) PEO and b) POEM chains in POEM9-5 (triangles), POEM5-7 (diamonds), and POEM2-8 (circles) blends with overall salt concentration of $r = 0.1$.

While solutions to Eqs 3-5 were found for all blend compositions for POEM9-5, POEM5-7, and POEM5-4, this was not the case for the POEM2 blends. The 25/75 and 50/50 blends did not yield real solutions. This is likely because there is very little, if any, LiTFSI solvated by the POEM2 chains, and so the favorable value for r_{POEM} is zero in these blends. This is further supported by the real solution found for the 75/25 blend prepared with POEM2-8, which was $r_{POEM} = 0.0029$ and $r_{PEO} = 0.13$ indicating a negligible amount of salt being solvated by POEM2. The r_{PEO} values assuming all LiTFSI is solvated by PEO, i.e., $r_{POEM} = 0$, for the 25/75 and 50/50 blends would be

r_{PEO} = 0.40 and 0.20, respectively. Previous studies have shown that PEO/LiTFSI at r = 0.40 is semi-crystalline.[13] Therefore, we will discuss the behavior of the 50/50 and 75/25 blends. If we compare the T_g values for the 75/25 and 50/50 blends to those of PEO/LiTFSI electrolytes at analogous r_{PEO} values assuming r_{POEM} = 0, we see good agreement (See Figure S35). For example, at r = 0.13 the T_g of PEO/LiTFSI is -33.8 ºC which agrees well with the measured T_g value for the 75/25 blend (-32.6 ºC). Likewise, at r = 0.20 the T_g of PEO/LiTFSI is -30.2 ºC, which is close to that of the 50/50 blend (-26.5 ºC). Therefore, we believe there is a negligible amount of salt solvated by POEM2 at all blend compositions. This is unsurprising as POEM2 has very short side chains, making it difficult for one individual chain to solvate a Li ion. Similar behavior is seen in blends prepared with POEM2-3 as shown in Figure S35.

In order to measure the ion transport properties, variable temperature electrochemical impedance spectroscopy (EIS) measurements were completed on all r = 0.1 electrolytes for temperatures ranging from 30 – 110 ºC. **Figure 4** shows the ionic conductivities for all homopolymers with r = 0.1 denoted with markers as a function of inverse temperature with the solid lines showing fit to the Vogel-Tamman-Fulcher (VTF) equation according to[21]

$$\sigma = \frac{A}{T^{1/2}} exp\left(\frac{-E_a}{R(T-T_o)}\right) \quad (5)$$

where σ is ionic conductivity, A is a fitted prefactor, T is the absolute temperature, T_o is equal to T_g – 50, R is the universal gas constant, and E_a is the fitted activation energy. The error bars on the data represent the standard deviations taken from triplicate samples. PEO exhibits a higher ionic conductivity than all of the POEM variants. The ionic conductivity was a strong function of POEM monomer structure with ionic conductivity increasing with increasing side chain length as reported previously.[26,27] The effect of molecular weight on ionic conductivity was less pronounced and was

shown to increase with increasing molecular weight for each specific POEM monomer (*e.g.,* the ionic conductivity for POEM5-7 was greater than that for POEM5-4). Furthermore, all of the homopolymer electrolytes displayed VTF behavior at all temperatures tested, and the fitted values for E_a were found to align with previous values reported in literature for PEO/LiTFSI.[4] The values for all fitted parameters in Eq 5 are provided in the Supporting Information (Table S2).

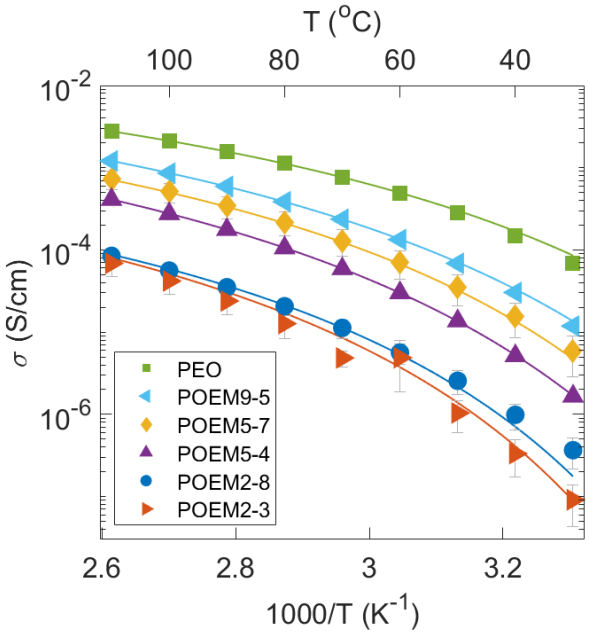

Figure 4. Ionic conductivity of PEO and all POEM homopolymers with $r = 0.1$ (markers) with the VTF fits (solid lines). Error bars show standard deviation in conductivity replicates.

Next, we examine the ion transport properties for the polymer blend electrolytes. **Figure 5** a), b), and c) show the ionic conductivity data in markers and the VTF fits in solid lines as a function of inverse temperature for the blends prepared with POEM2-8, POEM5-7, and POEM9-5, respectively. The error bars show the standard deviation from triplicates. For all POEM variants, the ionic conductivity of the blends increases with increasing PEO composition. However, the quantitative changes with blend composition are dependent on the molecular structure of the POEM monomer.

Although the ionic conductivity of blends prepared with POEM2-8 appears proportional to blending ratio on the log-scale plot presented in **Figure 5a,** the presence of the POEM2-8 polymers decreases the ion transport of the blends to a greater extent than would be expected based on the salt partitioning alone, **Figure 3**. For example, the ionic conductivity of the 25/75 blend at 90 ºC is 5.3% of that of PEO/LiTFSI at $r = 0.1$. If the POEM moieties were simply not participating in ion transport due to the salt being solvated solely by PEO, we would expect the resulting ionic conductivity to be that of PEO/LiTFSI at the salt concentration calculated in **Figure 3a** (*i.e.,* $r = 0.13$ for the 25/75 blend with POEM2-8). This would indicate that only the PEO moieties are transporting the Li ions as no salt is being solvated by the POEM2-8 polymers. Previous work has found that the ionic conductivity of PEO/LiTFSI at $r = 0.13$ is 1.2×10^{-3} S/cm, which is higher than what is found for the 25/75 blends studied here (8.4×10^{-4} S/cm).[37] This indicates that the presence of POEM2-8 chains decreases the ability of PEO to transport Li ions. In **Figure 5b,** we plot the ionic conductivity data for the blends prepared with POEM5-7 as a function of inverse temperature with comparisons to the reference homopolymers. Again, we see an increase in ionic conductivity with increasing PEO composition, but for this POEM variant, the ionic conductivity of the 75/25 blend is near that of pure PEO. Therefore, the POEM5-7 polymers must be contributing to the ion transport mechanism, which was not observed for the POEM2-8. If the POEM5-7 polymers were not participating in ion transport, we would assume that the ionic conductivity of the 75/25 blend would be approximately 75% of that of PEO/LiTFSI as described by effective medium theory.[38] The ionic conductivity for the blends prepared with POEM9-5 shown in **Figure 5c** is similar to the blends prepared with POEM5-7, although the ionic conductivity for the 75/25 blend quantitatively matches that of PEO at all temperatures studied. The ionic conductivity data for POEM2-3 and POEM5-4 is provided in the SI (Figure S37 and S36) and the trends agree with that of the

higher molecular weight POEM samples for each POEM monomer. These results show that the POEM side chain length influences the ion transport mechanism within the blends with PEO and that the effect of side chain length in the blends is distinct from that of the pure homopolymers. We hypothesize that these deviations result from different Li ion solvation structures than can be formed between POEM and PEO that do not exist in the pure homopolymer systems. Therefore, we believe that engineering miscible polymer blends may provide an avenue for generating polymer electrolytes with higher ionic conductivities than that of PEO/LiTFSI.

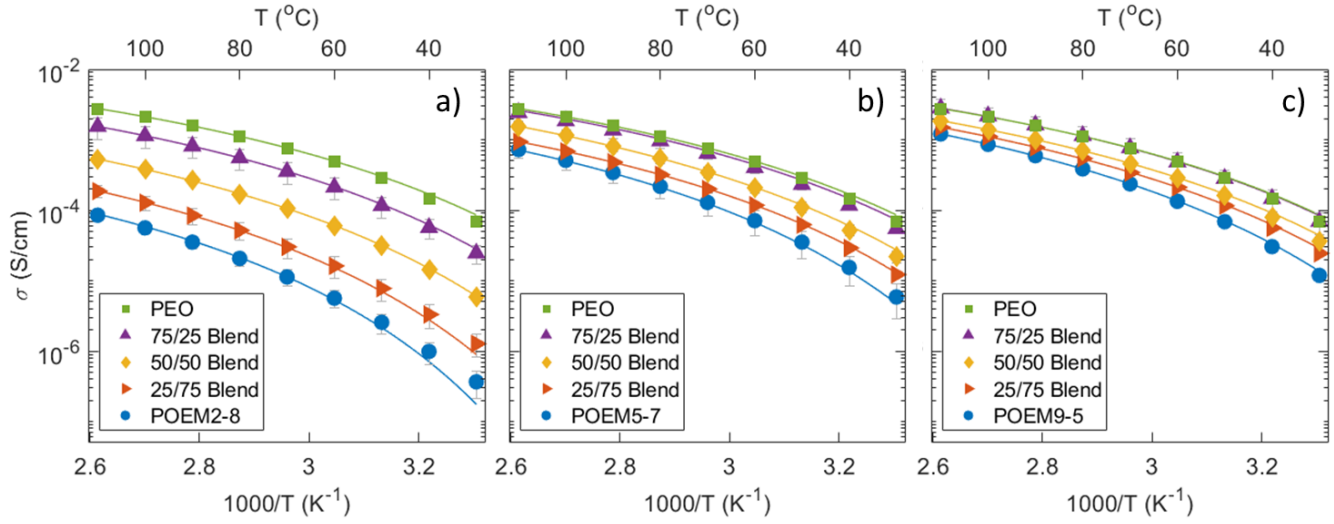

Figure 5. Conductivity values (markers) and VTF fits (solid lines) for a) POEM2-8, b) POEM5-7, and c) POEM9-5 polymer blend electrolytes with $r = 0.1$ for all electrolytes. Error bars show standard deviation of conductivity.

To further investigate the molecular mechanism behind the ionic conductivity, the reduced conductivity, σ_r was calculated using the fitting parameters, A and E_a, from the VTF fits (Eq 6) according to [4,39]

$$\sigma_r = \frac{A}{(Tg+110)^{1/2}} exp\left(\frac{-E_a}{R(160)}\right) \quad (6)$$

By calculating σ_r, we are able to quantify the ionic conductivity at a set value of 110 °C above the T_g of the blends, effectively comparing ion transport capabilities at a consistent degree of segmental dynamics. If changes in segmental dynamics were the only factor in influencing ionic conductivity in our blends, then plots of σ_r with respect to blend composition would be flat. Therefore, we can assume that any changes in σ_r with respect to blend composition can be attributed to some differences in solvation site environment that impact the motion of the ions.[4,39] **Figure 6** a), b), and c) show the σ_r as a function of w_{PEO} for blends prepared with POEM2-8, POEM5-7, and POEM9-5, respectively. POEM2-8 (**Figure 6a**) shows a monotonic increase in σ_r with increased w_{PEO}. This indicates that the presence of POEM2-8 decreases the ion solvation site connectivity and upon further addition of PEO to the blends, the Li solvation environment becomes more connected. This agrees with our previous conclusions that the presence of PEOM2-8 is negatively impacting the ion transport capabilities of PEO within the blend. While the solvation site connectivity increases with increasing w_{PEO} as evident by increasing σ_r values, the value of σ_r for the 75/25 blend is still significantly lower than that of pure PEO. Blends prepared with POEM2-3 behave quantitatively similar (Figure S38a). Conversely, while the values of σ_r increase with increasing w_{PEO} for POEM5-7 (**Figure 6b**) and POEM9-5 (**Figure 6c**) the magnitude of change is within one order of magnitude, significantly less than that of POEM2-8. In fact, all of the blends for POEM5-7 and POEM9-5 exhibit equal or greater values of σ_r compared to the 75/25 blend of POEM2-8. This indicates that the changes in segmental dynamics for the blends are the main contributor to changes in the ionic conductivity and that the solvation site structure remains fairly constant across the blend composition window. Interestingly, the σ_r value for blends prepared with POEM5-7 at compositions of 25/75 (**Figure 6b**) show a slightly lower value of σ_r than the POEM5-7 homopolymer. We hypothesize that this is due to the previously described co-solvation between

PEO and POEM which reduces the solvation site connectivity. However, when the PEO composition is increased to 75/25, σ_r is the same as that of the PEO homopolymer, indicating improved ion solvation site connectivity within the system. Blends prepared with POEM5-4 show similar trends for the behavior of reduced conductivity with respect to blend ratio (Figure S38b). The σ_r values for blends prepared with POEM9-5 (**Figure 6c**) increase with increasing w_{PEO} although the change in magnitude is fairly small. The reduced conductivity shows a similar behavior as that of the POEM5-7 blends but with the 50/50 being slightly higher than the POEM9-5 homopolymer and the 25/75 blend electrolytes. This is unsurprising as POEM9-5 solvates the ions more similar to PEO compared to other POEM variations, as a single POEM9 monomer can solvate a Li ion independently. Therefore, the ion solvation connectivity for blends prepared with POEM9-5 should be similar to that of pure PEO. It is interesting that POEM5-7 displays such similar behavior given its shorter side chain lengths that have more difficulty solvating the ions. Further investigations into the behavior of blends prepared with POEM5 polymers are necessary to develop a molecular understanding of the observed phenomenon. Overall, these results indicate that the solvation site structure and its connectivity, can be engineered by tuning blend properties, such as composition and monomer molecular structure, to generate electrolytes that are more advantageous for ion transport than that of pure PEO.

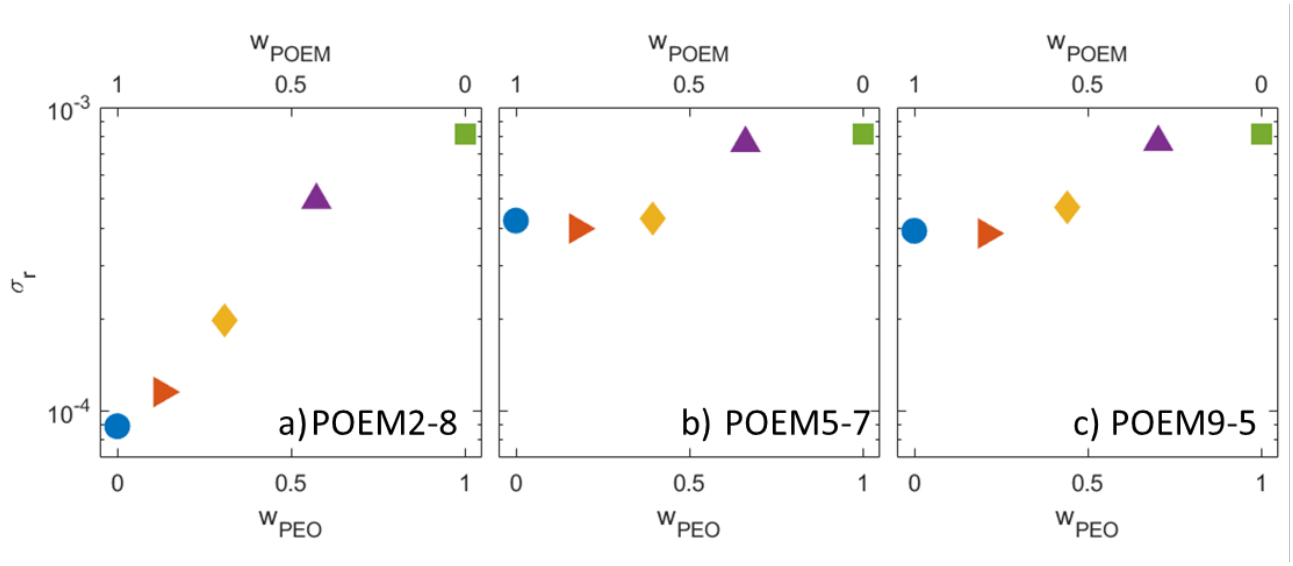

Figure 6. Reduced conductivity of a) POEM2-8, b) POEM5-7, and c) POEM5-9 blends with r = 0.1.

Conclusion

In this study, we show that the behavior of the PEO/POEM/LiTFSI polymer blend electrolyte systems is primarily affected by the POEM monomer structure characterized by side chain length. All PEO/POEM blends were miscible as indicated by the presence of one T_g in the DSC traces with and without salt. The salt free blends exhibited ideal mixing behavior predicted by the Fox Equation. Upon the addition of LiTFSI, all of the homopolymers had higher T_g values than PEO at r = 0.1, indicating that POEM is more affected by the presence of LiTFSI than PEO. Additionally, all electrolyte blends showed negative deviation from the Fox equation due to uneven salt partitioning withing the system. Upon further analysis, we found that Li is preferentially solvated by PEO versus POEM. In the blends prepared with POEM2, the POEM2 did not contribute to ion solvation indicating that the short side chains greatly reduce its ability to create a sufficient solvation

environment. These trends were further confirmed through measurements of the ionic conductivity. We found that homopolymer ionic conductivity was impacted significantly by POEM side chain length and, to a lesser extent, POEM molecular weight. When blended with PEO, all of the conductivities for the blends fell between that of the relevant POEM and PEO, with the exception of the 75/25 PEO/POEM9-5 blend which was the same as the pure PEO electrolyte. When we considered the reduced conductivity to quantify the effect of segmental dynamics of ion transport, we found that the connectivity of solvation sites was much lower in POEM2-8 and gradually increased with PEO content. The reduced conductivity for the blends prepared with POEM9-5 and POEM5-7 were qualitatively constant with respect to blend composition indicating that differences in segmental dynamics were the main contributor to differences in the ionic conductivity. Overall, we show that solvation site structure and segmental dynamics can be precisely tuned by changing blend properties, such as composition and monomer molecular structure, to generate electrolytes with improved ion transport properties compared to PEO/LiTFSI. Future work is required to investigate how co-solvation of Li ions between PEO and POEM can be leveraged to increase blend segmental dynamics and improve solvation site connectivity to generate high-performing electrolytes for next-generation rechargeable batteries.

Supporting Information

The Supporting Information (SI) contains structural characterization including GPC and NMR as well as the thermal characterization in the form of DSC scans for all polymer blends. The fits for T_g as a function of r for all homopolymers as well as thermal and electrochemical characterization of the POEM5-4 and POEM2-3 blends are also shown in the SI. The dataset for this study can be found at DOI: 10.6084/m9.figshare.29168405.

Acknowledgements

This research was primarily supported by NSF through the University of Wisconsin Materials Research Science and Engineering Center (DMR-2309000). The authors gratefully acknowledge use of facilities and instrumentation in the UW-Madison Wisconsin Center for Nanoscale Technology. The Center (wcnt.wisc.edu) is partially supported by the Wisconsin Materials Research Science and Engineering Center (NSF DMR-2309000) and the University of Wisconsin-Madison. The Bruker AVANCE III 500 NMR spectrometer was supported by a generous gift from Paul J. and Margaret M. Bender. The authors also thank the Boydston Lab in the Chemistry Department of University of Wisconsin-Madison for use of instrumentation.

Acronyms

LIBs = Lithium-Ion Batteries

SPE = Solid Polymer Electrolyte

PEO = poly(ethylene oxide)

EO = ethylene oxide

PEG = poly(ethylene glycol)

PMMA = poly(methyl methacrylate)

POEM = poly(oligo ethylene oxide methacrylate)

RAFT = reversible addition-fragmentation chain-transfer

DSC = Differential scanning calorimitry

EIS = electrochemical impedance spectroscopy

T_g = Glass transition temperature

r = salt concentration [Li]/[EO]

VTF = Vogel-Tamman-Fulcher

σ = ionic conductivity

T_o = Vogel Temperature, T_g – 50

A = VTF prefactor

E_a = activation energy

R = universal gas constant

σ_r = reduced conductivity

References

(1) Tarascon, J.-M.; Armand, M. Issues and Challenges Facing Rechargeable Lithium Batteries. *Nature* **2001**, *414* (6861), 359–367. https://doi.org/10.1038/35104644.

(2) Xue, Z.; He, D.; Xie, X. Poly(Ethylene Oxide)-Based Electrolytes for Lithium-Ion Batteries. *J. Mater. Chem. A* **2015**, *3* (38), 19218–19253. https://doi.org/10.1039/C5TA03471J.

(3) Endo, A.; Tsurita, I.; Burnett, K.; Orencio, P. M. A Review of the Current State of Research on the Water, Energy, and Food Nexus. *J. Hydrol. Reg. Stud.* **2017**, *11*, 20–30. https://doi.org/10.1016/j.ejrh.2015.11.010.

(4) Zheng, Q.; Pesko, D. M.; Savoie, B. M.; Timachova, K.; Hasan, A. L.; Smith, M. C.; Miller, T. F. I.; Coates, G. W.; Balsara, N. P. Optimizing Ion Transport in Polyether-Based Electrolytes for Lithium Batteries. *Macromolecules* **2018**, *51* (8), 2847–2858. https://doi.org/10.1021/acs.macromol.7b02706.

(5) Wang, J.; Ge, B.; Li, H.; Yang, M.; Wang, J.; Liu, D.; Fernandez, C.; Chen, X.; Peng, Q. Challenges and Progresses of Lithium-Metal Batteries. *Chem. Eng. J.* **2021**, *420*, 129739. https://doi.org/10.1016/j.cej.2021.129739.

(6) Varzi, A.; Thanner, K.; Scipioni, R.; Di Lecce, D.; Hassoun, J.; Dörfler, S.; Altheus, H.; Kaskel, S.; Prehal, C.; Freunberger, S. A. Current Status and Future Perspectives of Lithium Metal Batteries. *J. Power Sources* **2020**, *480*, 228803. https://doi.org/10.1016/j.jpowsour.2020.228803.

(7) Nair, J. R.; Imholt, L.; Brunklaus, G.; Winter, M. Lithium Metal Polymer Electrolyte Batteries: Opportunities and Challenges. *Electrochem. Soc. Interface* **2019**, *28* (2), 55. https://doi.org/10.1149/2.F05192if.

(8) Ghelichi, M.; Qazvini, N. T.; Jafari, S. H.; Khonakdar, H. A.; Farajollahi, Y.; Scheffler, C. Conformational, Thermal, and Ionic Conductivity Behavior of PEO in PEO/PMMA Miscible Blend: Investigating the Effect of Lithium Salt. *J. Appl. Polym. Sci.* **2013**, *129* (4), 1868–1874. https://doi.org/10.1002/app.38897.

(9) Gorecki, W.; Jeannin, M.; Belorizky, E.; Roux, C.; Armand, M. Physical Properties of Solid Polymer Electrolyte PEO(LiTFSI) Complexes. *J. Phys. Condens. Matter* **1995**, *7* (34), 6823. https://doi.org/10.1088/0953-8984/7/34/007.

(10) Yang, H.; Wu, N. Ionic Conductivity and Ion Transport Mechanisms of Solid-State Lithium-Ion Battery Electrolytes: A Review. *Energy Sci. Eng.* **2022**, *10* (5), 1643–1671. https://doi.org/10.1002/ese3.1163.

(11) Fenton, D. E.; Parker, J. M.; Wright, P. V. Complexes of Alkali Metal Ions with Poly(Ethylene Oxide). *Polymer* **1973**, *14* (11), 589. https://doi.org/10.1016/0032-3861(73)90146-8.

(12) Gao, K. W.; Balsara, N. P. Electrochemical Properties of Poly(Ethylene Oxide) Electrolytes above the Entanglement Threshold. *Solid State Ion.* **2021**, *364*, 115609. https://doi.org/10.1016/j.ssi.2021.115609.

(13) Grundy, L. S.; Fu, S.; Hoffman, Z. J.; Balsara, N. P. Electrochemical Characterization of PEO/LiTFSI Electrolytes Near the Solubility Limit. *Macromolecules* **2022**, *55* (20), 9030–9038. https://doi.org/10.1021/acs.macromol.2c01655.

(14) Bakar, R.; Darvishi, S.; Li, T.; Han, M.; Aydemir, U.; Nizamoglu, S.; Hong, K.; Senses, E. Effect of Polymer Topology on Microstructure, Segmental Dynamics, and Ionic Conductivity in PEO/PMMA-Based Solid Polymer Electrolytes. *ACS Appl. Polym. Mater.* **2022**, *4* (1), 179–190. https://doi.org/10.1021/acsapm.1c01178.

(15) Aldalur, I.; Martinez-Ibañez, M.; Krztoń-Maziopa, A.; Piszcz, M.; Armand, M.; Zhang, H. Flowable Polymer Electrolytes for Lithium Metal Batteries. *J. Power Sources* **2019**, *423*, 218–226. https://doi.org/10.1016/j.jpowsour.2019.03.057.
(16) Aziz, S. B.; Woo, T. J.; Kadir, M. F. Z.; Ahmed, H. M. A Conceptual Review on Polymer Electrolytes and Ion Transport Models. *J. Sci. Adv. Mater. Devices* **2018**, *3* (1), 1–17. https://doi.org/10.1016/j.jsamd.2018.01.002.
(17) Marzantowicz, M.; Krok, F.; Dygas, J. R.; Florjańczyk, Z.; Zygadło-Monikowska, E. The Influence of Phase Segregation on Properties of Semicrystalline PEO:LiTFSI Electrolytes. *Solid State Ion.* **2008**, *179* (27), 1670–1678. https://doi.org/10.1016/j.ssi.2007.11.035.
(18) Kelly, I.; Owen, J. R.; Steele, B. C. H. Mixed Polyether Lithium-Ion Conductors. *J. Electroanal. Chem. Interfacial Electrochem.* **1984**, *168* (1), 467–478. https://doi.org/10.1016/0368-1874(84)87116-6.
(19) Chintapalli, S.; Frech, R. Effect of Plasticizers on Ionic Association and Conductivity in the (PEO)9LiCF3SO3 System. *Macromolecules* **1996**, *29* (10), 3499–3506. https://doi.org/10.1021/ma9515644.
(20) Frech, R.; Chintapalli, S. Effect of Propylene Carbonate as a Plasticizer in High Molecular Weight PEO□LiCF3SO3 Electrolytes. *Solid State Ion.* **1996**, *85* (1), 61–66. https://doi.org/10.1016/0167-2738(96)00041-0.
(21) Zhu, C.; Pedretti, B. J.; Kuehster, L.; Ganesan, V.; Sanoja, G. E.; Lynd, N. A. Ionic Conductivity, Salt Partitioning, and Phase Separation in High-Dielectric Contrast Polyether Blends and Block Polymer Electrolytes. *Macromolecules* **2023**, *56* (3), 1086–1096. https://doi.org/10.1021/acs.macromol.2c02023.
(22) Choo, Y.; Halat, D. M.; Villaluenga, I.; Timachova, K.; Balsara, N. P. Diffusion and Migration in Polymer Electrolytes. *Prog. Polym. Sci.* **2020**, *103*, 101220. https://doi.org/10.1016/j.progpolymsci.2020.101220.
(23) Gao, K. W.; Loo, W. S.; Snyder, R. L.; Abel, B. A.; Choo, Y.; Lee, A.; Teixeira, S. C. M.; Garetz, B. A.; Coates, G. W.; Balsara, N. P. Miscible Polyether/Poly(Ether–Acetal) Electrolyte Blends. *Macromolecules* **2020**, *53* (14), 5728–5739. https://doi.org/10.1021/acs.macromol.0c00747.
(24) Shah, N. J.; Shalaby, M.; He, L.; Wang, X.; Deslandes, D.; Garetz, B. A.; Balsara, N. P. Chimney-Shaped Phase Diagram in a Polymer Blend Electrolyte. *ACS Macro Lett.* **2023**, *12* (7), 874–879. https://doi.org/10.1021/acsmacrolett.3c00285.
(25) Shah, N. J.; He, L.; Gao, K. W.; Balsara, N. P. Thermodynamics and Phase Behavior of Poly(Ethylene Oxide)/Poly(Methyl Methacrylate)/Salt Blend Electrolytes Studied by Small-Angle Neutron Scattering. *Macromolecules* **2023**, *56* (7), 2889–2898. https://doi.org/10.1021/acs.macromol.2c02533.
(26) Bennington, P.; Deng, C.; Sharon, D.; A. Webb, M.; Pablo, J. J. de; F. Nealey, P.; N. Patel, S. Role of Solvation Site Segmental Dynamics on Ion Transport in Ethylene-Oxide Based Side-Chain Polymer Electrolytes. *J. Mater. Chem. A* **2021**, *9* (15), 9937–9951. https://doi.org/10.1039/D1TA00899D.
(27) Deng, C.; Webb, M. A.; Bennington, P.; Sharon, D.; Nealey, P. F.; Patel, S. N.; de Pablo, J. J. Role of Molecular Architecture on Ion Transport in Ethylene Oxide-Based Polymer Electrolytes. *Macromolecules* **2021**, *54* (5), 2266–2276. https://doi.org/10.1021/acs.macromol.0c02424.
(28) Sharon, D.; Deng, C.; Bennington, P.; Webb, M. A.; Patel, S. N.; de Pablo, J. J.; Nealey, P. F. Critical Percolation Threshold for Solvation-Site Connectivity in Polymer Electrolyte

Mixtures. *Macromolecules* **2022**, *55* (16), 7212–7221. https://doi.org/10.1021/acs.macromol.2c00988.
(29) Colmenero, J.; Arbe, A. Segmental Dynamics in Miscible Polymer Blends: Recent Results and Open Questions. *Soft Matter* **2007**, *3* (12), 1474–1485. https://doi.org/10.1039/B710141D.
(30) He, Y.; Lutz, T. R.; Ediger, M. D. Segmental and Terminal Dynamics in Miscible Polymer Mixtures: Tests of the Lodge–McLeish Model. *J. Chem. Phys.* **2003**, *119* (18), 9956–9965. https://doi.org/10.1063/1.1615963.
(31) Hiemenz, P. C.; Lodge, T. P. *Polymer Chemistry, Second Edition*; Taylor & Francis, 2007.
(32) Kalogeras, I. M.; Brostow, W. Glass Transition Temperatures in Binary Polymer Blends. *J. Polym. Sci. Part B Polym. Phys.* **2009**, *47* (1), 80–95. https://doi.org/10.1002/polb.21616.
(33) Feldstein, M. M.; Shandryuk, G. A.; Platé, N. A. Relation of Glass Transition Temperature to the Hydrogen-Bonding Degree and Energy in Poly(*N*-Vinyl Pyrrolidone) Blends with Hydroxyl-Containing Plasticizers. Part 1. Effects of Hydroxyl Group Number in Plasticizer Molecule. *Polymer* **2001**, *42* (3), 971–979. https://doi.org/10.1016/S0032-3861(00)00445-6.
(34) Shenogin, S.; Kant, R.; Colby, R. H.; Kumar, S. K. Dynamics of Miscible Polymer Blends: Predicting the Dielectric Response. *Macromolecules* **2007**, *40* (16), 5767–5775. https://doi.org/10.1021/ma070503q.
(35) Tran-Cong, Q.; Nakano, H.; Okinaka, J.; Kawakubo, R. Miscibility of Poly(2-Chlorostyrene) and Poly(Vinyl Methyl Ether) Blends. *Polymer* **1994**, *35* (6), 1242–1247. https://doi.org/10.1016/0032-3861(94)90018-3.
(36) Diddens, D.; Heuer, A.; Borodin, O. Understanding the Lithium Transport within a Rouse-Based Model for a PEO/LiTFSI Polymer Electrolyte. *Macromolecules* **2010**, *43* (4), 2028–2036. https://doi.org/10.1021/ma901893h.
(37) Mongcopa, K. I. S.; Tyagi, M.; Mailoa, J. P.; Samsonidze, G.; Kozinsky, B.; Mullin, S. A.; Gribble, D. A.; Watanabe, H.; Balsara, N. P. Relationship between Segmental Dynamics Measured by Quasi-Elastic Neutron Scattering and Conductivity in Polymer Electrolytes. *ACS Macro Lett.* **2018**, *7* (4), 504–508. https://doi.org/10.1021/acsmacrolett.8b00159.
(38) Galluzzo, M. D.; Loo, W. S.; Wang, A. A.; Walton, A.; Maslyn, J. A.; Balsara, N. P. Measurement of Three Transport Coefficients and the Thermodynamic Factor in Block Copolymer Electrolytes with Different Morphologies. *J. Phys. Chem. B* **2020**, *124* (5), 921–935. https://doi.org/10.1021/acs.jpcb.9b11066.
(39) Pesko, D. M.; Webb, M. A.; Jung, Y.; Zheng, Q.; Miller, T. F. I.; Coates, G. W.; Balsara, N. P. Universal Relationship between Conductivity and Solvation-Site Connectivity in Ether-Based Polymer Electrolytes. *Macromolecules* **2016**, *49* (14), 5244–5255. https://doi.org/10.1021/acs.macromol.6b00851.

For Table of Contents Only: